

# Design and performance of a new compact adaptable autostigmatic alignment tool

William P. Kuhn

Opt-E, 3450 S Broadmont Dr Ste 112, Tucson, AZ, USA 85713-5245

[bill.kuhn@opt-e.com](mailto:bill.kuhn@opt-e.com)

## ABSTRACT

The design and performance of a compact, adaptable autostigmatic alignment module that can be used as an autocollimator or autostigmatic microscope is described. The new instrument utilizes LED illumination and reticle projection and is compared with a laser diode based point source microscope. Measurement characteristics and practical differences and similarities between the instruments are described.

**Keywords:** autostigmatic microscope, autocollimator, optical alignment, adaptable alignment module, point source microscope

## 1. INTRODUCTION

Autostigmatic alignment tools are in common use for alignment and metrology of optical and mechanical systems. The autocollimator is the classical tool for alignment tasks at infinite conjugates involving flat optics or a collimated wavefront. The autocollimator is the common name for an autostigmatic telescope. Autocollimators in conjunction with auxiliary optics can be used for a variety of tasks including alignment of linear stage axes or finding the axis of rotation of a bearing. The autostigmatic microscope is a finite conjugate autostigmatic alignment tool and is sometimes referred to as a point source microscope (PSM). Autostigmatic microscopes are useful for locating optics via their center-of-curvature, while autocollimators locate the surface normal of flat optics.

Autostigmatic instruments project a target to the corresponding conjugate – infinite or finite – and produce a return image on a camera, position sensing detector or the reticle of an eyepiece. The target may be a point source, crosshair or other reticle. A reference location is established by some means (e.g. cat's eye image or retro-reflection) and the instrument is used to measure the distance or angle between the return image location and reference position and to set focus.

A new, compact, adaptable autostigmatic alignment tool has been developed that can be used as either an electronic autocollimator or autostigmatic microscope. The instrument uses LED illumination and a novel reticle design to provide improved performance compared to a laser diode based point source. The autostigmatic alignment module features are described and its performance is evaluated.

## 2. DESIGN

### 2.1 History

The author<sup>[1]</sup> designed a point source microscope a number of years ago. The instrument, called the PSM, integrated a fiber-coupled laser diode and a full-field illumination system into a rugged, compact body. The PSM has been used successfully as a small beam autocollimator, an autostigmatic microscope, and even an interference microscope. The instrument is basically an infinite conjugate microscope with both full-field illumination and a point source.

At the time the PSM was designed 1/3" format CCD cameras were just becoming available in small packages with Firewire interfaces (IEEE-1394) that could be connected to notebook computers. The initial camera selected was a Point Grey Flea-HIBW camera with 1024 x 768 pixels of 4.65  $\mu\text{m}$  height and width. Similarly, compact fiber-coupled laser diodes were available that could provide a bright, "find-it" beam, as well as a dim spot for final alignment. The dim mode of operation has reduced coherence length, which is generally preferable for alignment tasks.

The mode-field diameter of a single-mode fiber for red light (~635 nm) is about 4  $\mu\text{m}$ . However, a spot this size on a detector with 4.65  $\mu\text{m}$  pixels would lead to a very badly quantized estimate of the spot lateral position. As a result, the design incorporated a short focal length collimator (around 35 mm) for the fiber output and a 100 mm focal length tube lens for the camera. The fiber output is thereby magnified onto the camera by about a factor of three, providing some extent to the spot for calculating the spot centroid. Increasing the size of the spot would improve the estimate of the lateral position while concurrently decreasing the field-of-view (FOV) of the instrument. A large FOV is desirable to facilitate finding the beam at all. The balance between FOV and spot size is the core trade-off in the PSM's design.

As a practical note, a 100 mm focal length cemented achromatic doublet has reasonable image quality up to about 0.5 degrees off-axis at around F/5<sup>[2]</sup>. However, if you are operating at F/10 or F/15 and quasi-monochromatically image quality more that is more than adequate to see a spot for initial alignment exists out to nearly 2 degrees off-axis. A 100 mm focal length lens and sensor with a 6 mm diagonal meets this loosely defined constraint.

Once the PSM design evolved to a camera with a tube lens, it looked like an infinite conjugate microscope. This realization led to the addition of a full-field illuminator to facilitate finding fiducial marks or for use as a reflected light microscope or even interference microscope. Packaging constraints, camera costs and of course, schedule and budget, led to a trade-off that resulted in good illumination uniformity over a 1/3" format sensor with typical dimensions 4.8 mm x 3.6 mm. However, the full field illumination system is not particularly well suited to larger format sensors, which were not a practical option at that time.

## 2.2 Motivation for a new design

The author recently designed a compact reflected light microscope (W1) with improved illumination over a larger FOV than the PSM. The W1 is essentially the same length and height as the PSM, but a bit thicker to accommodate larger optics. Larger optics are required to implement a telecentric microscope illumination system (Köhler) supporting larger FOV cameras. Additionally, internal electronics includes a USB2 interface to power and to control the light source. The electronics appear as a virtual COM port in a computer. The electronics in the W1 include multiple, digitally controlled current sources with voltage compliance sufficient to drive blue and white LEDs reliably using power from the USB2 port. The current sources can be connected in parallel for more current or used to drive multiple LEDs. The W1 exceeds the PSM capabilities as a reflected light microscope; however, it has only full-field illumination for use as a microscope. The W1 does not have a point source to function as an alignment tool.



Figure 1. W1 reflected light microscope with C-mount camera on the left and PZT mount on the right. The PZT mount can be used for focusing as well as phase-shifting interferometry or coherence scanning interferometry. A standard RMS objective is attached.

Attempts to adapt the W1 design into an alignment tool were inconvenient largely due to the trade-off between FOV and spot size that exists in the PSM design. Given the experience with the improved electronics and Köhler illumination system in the W1 a different design path was considered for an alignment tool. Specifically, build a slide projector so as to decouple the diffraction limited point source useful for qualitative assessment of aberrations from a larger feature used for centroid calculations.

## 2.3 Notional design elements

Once the idea of a slide projector arose, the design progressed quickly. The electronics from the W1 can be used providing linear and fine control of the light source. Using an LED, instead of a laser diode, removes laser safety

requirements. It also eliminates speckle. Since the features on the target can be printed at the same size as desired on the camera, magnification from source to detector is no longer required. This makes it possible to use a single lens as both the collimator for the light being sent out as well as the tube lens for the camera. This in turn leads to the use of a cube beam splitter on the target and detector side of the collimator. At F/10, the spherical aberration is negligible and longitudinal color does not matter for a relatively narrow band source.

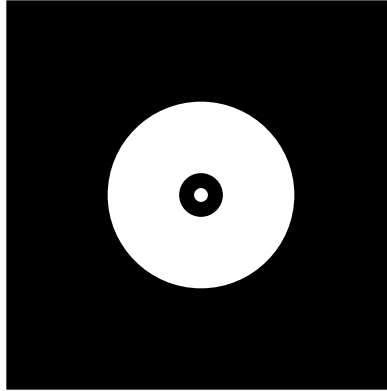


Figure 2. The reticle design is shown schematically, but is not to scale. The reticle functions as a field stop and is an opaque square in the schematic with a set of centered circles: a large aperture, a small obscuration and a still smaller aperture.

How to implement a “find-it” beam with an LED? Alternatively, how does one make use of the substantial optical power available from a small LED that is an extended, not point, source? The solution is the reticle design.

The nominal reticle design is a large, opaque square. Inside the square are a set of centered, concentric circular features. The large aperture might have a diameter about half the sensor width. The smaller opaque circle in the center is an obscuration that is used for centering via centroid calculations. Within the small obscuration is a hole, typically a hole whose diameter is about the diameter of the central Airy disk, or perhaps a bit smaller. The pinhole provides a diffraction limited point source for assessing image quality. The large aperture allows a substantial amount of light to be projected by the system and provides the “find-it” beam or spot function.

The reticle is a field stop, or essentially a slide that is being projected. The large aperture and small obscuration results in a substantial illuminated area allowing one to see fiducials or other features at the same time as the alignment features are present. The large aperture and point source, in addition to the obscuration, can also be used for centroid calculations.

## 2.4 Schematic layout

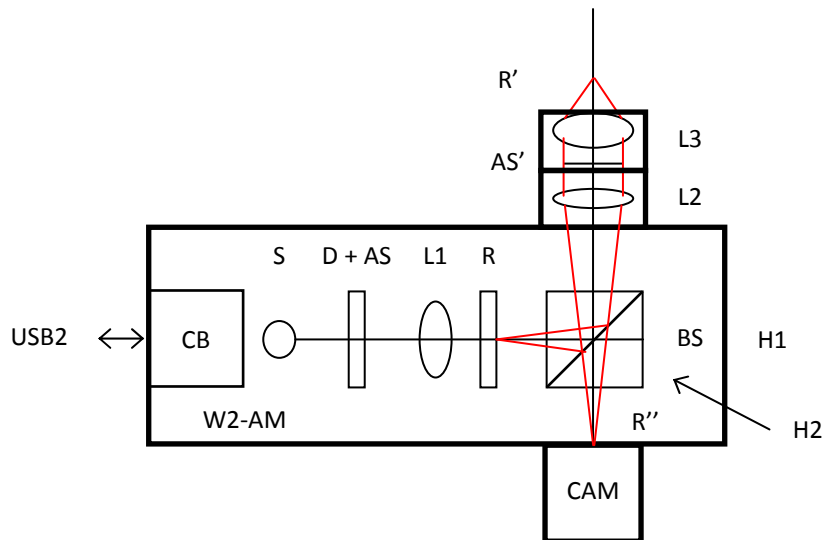


Figure 3. W2 alignment module schematic layout.

The schematic layout illustrates the essential features of the instrument. The components are as follows:

1. USB2 – computer connection,
2. CB – circuit board,
3. S – source LED,
4. D + AS – diffuser and aperture stop,
5. L1 – condenser lens,
6. R – reticle (field stop),
7. BS – 1” beam splitter cube,
8. L2 – collimating lens assembly,
9. AS’ – image of aperture stop,
10. L3 – optional focusing lens (e.g. microscope objective),
11. R’ – finite conjugate image of R with L3 installed, or at infinity without L3,
12. R’’ – image of reticle after projection and return, with or without L3,
13. CAM – C-mount camera,
14. H1 – hole pattern on enclosure side,
15. H2 – hole pattern on enclosure bottom, and
16. W2-AM – alignment module assembly and enclosure.

The core of the W2 optics is a Köhler illuminator and a cube beam splitter. The cube adds spherical aberration to a diverging or converging beam; however, at F/10 or slower, the aberration is negligible. The cube also adds longitudinal color, but the sources used are typically narrow band. Unlike a plate beam splitter, the cube does not add coma or astigmatism to a diverging or converging beam.

## 2.5 Package

The W2 package is made from an aluminum block and is 55 mm x 60 mm x 150 mm. Mounting patterns are on two sides as shown in the figure below and include metric (M6) and imperial (1/4”-20) tapped holes for flexibility on appropriate grids (25 mm and 1” respectively). Smaller threads sizes (e.g. M4, 8-32, etc.) can be obtained with catalog thread adapters. Additionally, 4-40 tapped holes on a 30 mm square are on the front and back for compatibility with cage mounting systems. C-mount cameras are mounted on the back to allow for selecting the appropriate camera for the application. The camera mount allows setting of camera clocking. The W2 is shown with a microscope objective attached to a 100 mm focal length collimator lens.

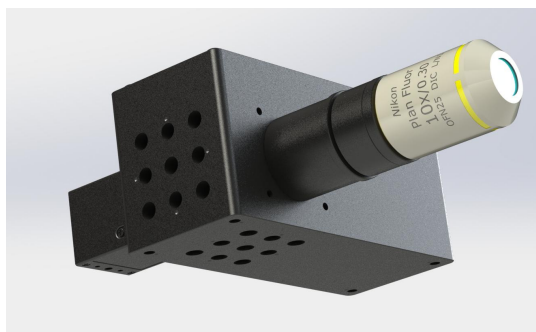


Figure 4. W2 alignment module with Nikon 10x objective. Removing the objective exposes a >10 mm diameter collimated beam when the standard 100 mm focal length collimating lens is installed

## 2.6 Adaptability

The W2 can be built to operate at wavelengths from the ultraviolet, through the visible and near-IR all the way through SWIR wavelengths (up to ~1.7  $\mu\text{m}$ ) in a fairly straight forward manner. Longer wavelengths pose additional issues yet to

be addressed. The optical elements and coatings can be selected to match the source wavelength at modest cost. Suitable cameras using silicon or InGaAs cameras can be used depending upon the source wavelength.

Additional flexibility arises in the collimator and optional focusing lenses. It is straightforward to build an instrument with a larger or smaller collimated beam since the core W2 alignment module is a diverging point source. Basically a different collimating lens is used with appropriate tubes. In many cases, catalog components can be used for this purpose. Alternatively, custom optics can be incorporated. For instance if one wants a telephoto collimator, or if color correction accounting for the beam splitter cube is desired, custom optics may be appropriate. Microscope objectives can certainly be used for finite conjugates tests as can other lenses depending upon the working distance, FOV, and numerical aperture required.

In addition to the optical flexibility, the mechanical package is easily integrated into setups. Similarly, the light source can be easily controlled from most any development environment through a virtual COM port. Finally, different reticles can be designed and integrated with application specific features, such as slanted edges for spatial frequency response calculations per ISO Standard 12233.

### 3. PERFORMANCE EVALUATION

#### 3.1 Overview

As a practical matter, the performance of the PSM is often limited more by the stability of the mounting fixtures or the environment than by the instrument itself. The same is likely to be true with the W2. Even so there are instrument characteristics of a practical nature to consider, as well as the limiting measurement performance of the instrument for both centroid (lateral position) and focus (axial position). Comparisons of both types of issues are made below.

#### 3.2 Centroid measurement

The measurement of a spot centroid is core to the W2's function, as well as the PSM. In order to remove the effect of the environment, a flat mirror was attached directly to a W2 prototype, and then a PSM. The same camera was used on each instrument to eliminate another difference. A simple automatic thresholding routine was used to identify a binary region corresponding to the "spot" of interest. For the PSM, the only spot is the point source. For the W2, the central, diffraction limited hole is essentially the same as the PSM source. Additionally, the centroid of the W2 obscuration and also its large aperture was found.

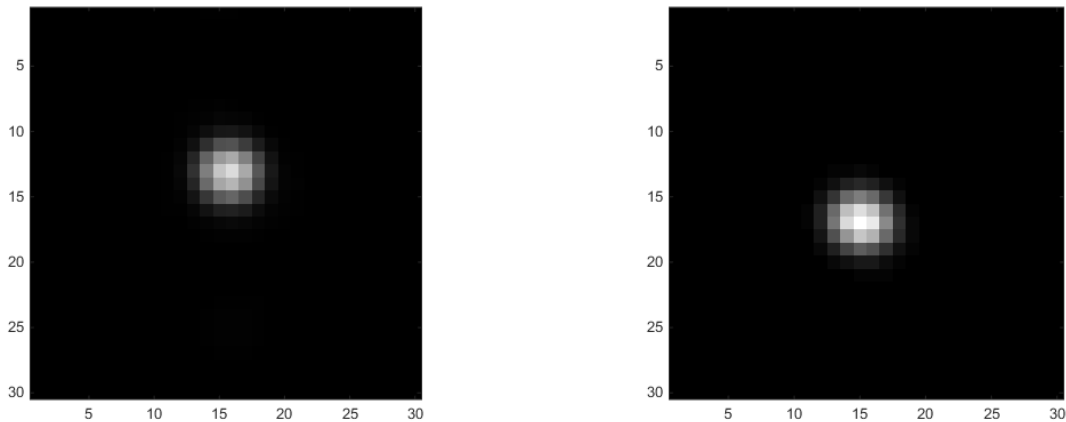


Figure 5. 30 x 30 pixel PSM spot image from fixed mirror. The mirror was rotated between the two images resulting in a different alignment of the spot to the pixel grid.

The measurement of interest is not in the absolute spot position, but rather, the variability of the spot position. For each of the four cases (PSM, W2-pinhole, W2-obscuration, and W2-large aperture) a series of 10 measurements was made. Each measurement in the set of 10 was comprised of 100 images where the centroid and area of the "blob" of interest in each image were calculated. The standard deviation of the centroid in X and Y and the area was calculated for each set of 100 images was also calculated.

The preceding figure shows a PSM spot for two different clocking positions of the mirror, which result in a different alignment of the spot to the pixel grid. This small change can affect the number of points included in the “blob” used for the centroid calculation. This is true for the W2 as well since it is due to position quantization effects of a small spot.

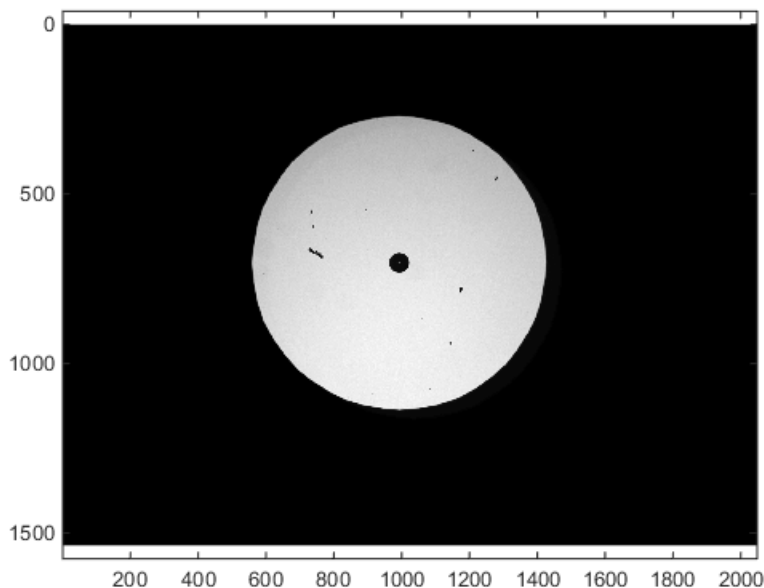


Figure 6. Full image from the W2 with a flat mirror fixed to the instrument. The reticle features a 3 mm diameter aperture, 200  $\mu\text{m}$  diameter obscuration and 14  $\mu\text{m}$  diameter aperture.

The preceding figure shows the full image from the W2. There is some debris in the large aperture of the prototype instrument. It will be removed in production. Even though the debris is aesthetically unappealing, it does not preclude the instrument from functioning as intended.

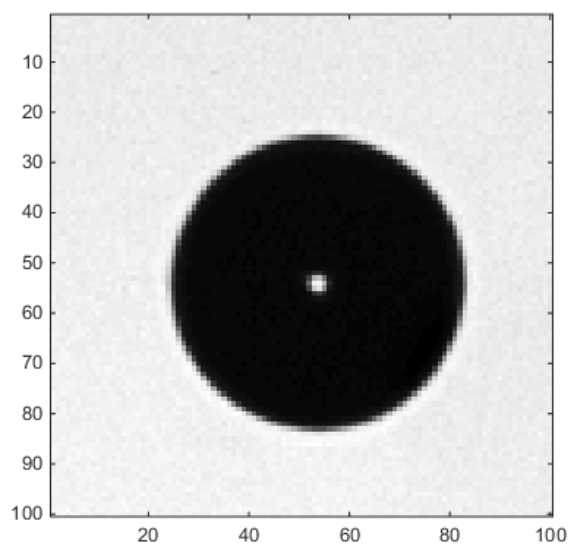


Figure 7. 100 x 100 pixel region from the W2 image above showing the central obscuration and central pinhole.

The central, 200  $\mu\text{m}$  diameter obscuration is clearly visible in the image above. It has reasonably sharp edges and is very circular.

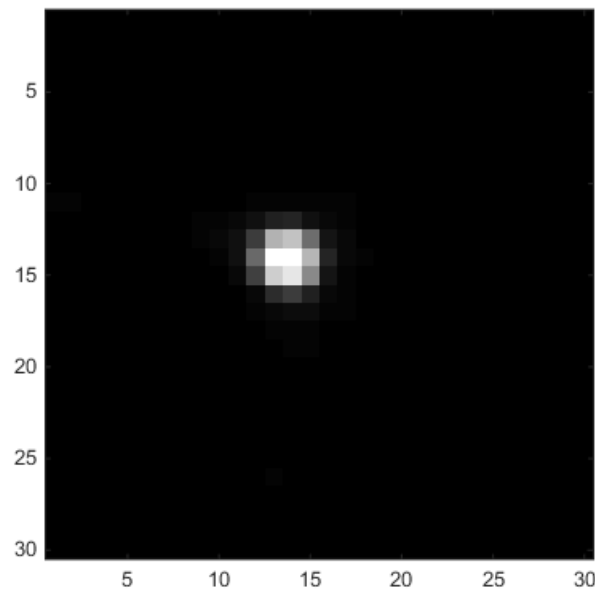


Figure 8. 30 x 30 pixel region from the W2 image above showing the central pinhole. The spot image is smaller than the PSM, because the system is operating at about F/10, instead of F/15 as an autocollimator.

The W2 pinhole image is smaller than the PSM image because the W2 with a 100 mm focal length lens and 10 mm diameter beam is operating at about F/10, instead of the PSM F/15 with a 100 mm focal length lens and a roughly 6.5 mm diameter beam. A further note that the W2 has nominally uniform illumination in the aperture, while the PSM has a Gaussian beam. Regardless of the beam type, calculating the centroid of the image from the small spot is subject to spatial quantization effects in both instruments.

Table 1. Minimum and maximum standard deviations from each measurement run for the PSM and the W2 pinhole.

	<b>PSM (1)</b>	<b>PSM (2)</b>	<b>W2 (1)</b>	<b>W2 (2)</b>
X (min)	0.0000	0.0787	0.0000	0.0000
Y (min)	0.0000	0.0425	0.0000	0.0000
Radial (min)	0.0000	0.0338	0.0000	0.0000
Area (min)	0.0000	0.5183	0.0000	0.0000
X (max)	0.0189	0.1188	0.0457	0.0815
Y (max)	0.0159	0.0556	0.0304	0.0543
Radial (max)	0.0239	0.0706	0.0460	0.0503
Area (max)	0.1414	0.6875	0.2739	0.4888
Mean area	9.99	9.47	8.99	8.15
Area std/mean	0.0142	0.0726	0.0305	0.0560

Each column of the preceding table summarizes the results from one of four series of 10 measurements. Each measurement in a series is the standard deviation of the particular property: X centroid, Y centroid, radial distance from mean centroid, and blob area. The minimum and maximum standard deviations are reported. The PSM and W2 each had a mirror rigidly fixed to the instrument for the measurement series. The mirror was rotated between (1) and (2) for each instrument to cause the spot to align differently to the pixel grid.

Interestingly, in multiple cases, there were measurements with a standard deviation of zero. However, the blob sizes were about 10 pixels each. Sometimes the same pixels were found resulting in a standard deviation of zero. However, just as easily, the standard deviations could be as large as 0.12 pixels for the PSM (X centroid) or 0.08 for the W2 (X centroid). One might argue the W2 performed slightly better than the PSM in this test, but the real issue is that a small spot has a potentially large quantization error resulting in somewhat unpredictable statistics. Even so, both tools can work well using data from just the small spot. Note that a standard deviation of 0.69 on pixel area of a 10 is a large fraction of the area. Increasing the area of the spot used in calculating a centroid can reduce the variability in the estimate of the centroid position.

Table 2. Minimum and maximum standard deviations from each measurement run for the W2 obscuration and large aperture.

	<b>W2-obs</b>	<b>W2-large</b>
X (min)	0.0032	0.0023
Y (min)	0.0072	0.0030
Radial (min)	0.0044	0.0018
Area (min)	0.8998	5.0674
X (max)	0.0094	0.0038
Y (max)	0.0108	0.0041
Radial (max)	1.0463	0.0222
Area (max)	1.2727	6.3476
Mean area	2670.66	588285
Area std/mean	0.0005	0.0000

The preceding table makes it clear that the size of the larger size of the obscuration improves the measurement by reducing the standard deviation compared to the small pinhole. There are no more “zeros”; however, the quantization error is greatly reduced. The large aperture is marginally better than the obscuration. The small improvement is probably due to the blurry edge of the large aperture in the image. The W2 obscuration has a standard deviation on centroid position of less than 0.01 pixels. For the 100 mm collimator lens with a camera having 3.45  $\mu\text{m}$  pixels this corresponds to  $(0.01 * 3.45 \mu\text{m}) / 100 \text{ mm} = 0.345 \mu\text{radians}$  standard deviation on angle measurements for a *single* centroid measurement. Averaging measurements could reduce this further. More sophisticated image processing (e.g. gray level rather than binary) could possibly reduce this still further.

### 3.3 Axial measurement

A very simple experiment was done where the operator (author) selected the best focus position visually. A micrometer head reading in 1  $\mu\text{m}$  increments was used to move the PSM and W2 axially about the center of a small, silicon nitride tooling ball. A 10x, NA 0.25 Olympus objective was used.

Table 3. The standard deviation in microns of the axial position of best focus

	<b>PSM</b>	<b>W2- pinhole</b>	<b>W2- edge</b>
STD axial position ( $\mu\text{m}$ )	0.919	0.994	0.675

The PSM standard deviation of 0.919  $\mu\text{m}$  for the axial position is a little better than the W2-pinhole. Using the sharpness of the edge of the W2 obscuration resulted in slightly better repeatability. Some effort is required to ensure that there is no bias on axial position by using the edge of the centroid. This experiment was performed with a 10x, NA 0.25 objective. Both instruments use the full NA of the objective, even though the W2 has a larger beam than the W2, but the objective limits the aperture size to be the practically the same for the two instruments. In some small number cases, a higher NA objective might provide an advantage for the W2.



Why does the PSM have a slight advantage over the W2-pinhole? There is a small amount of astigmatism in the PSM.

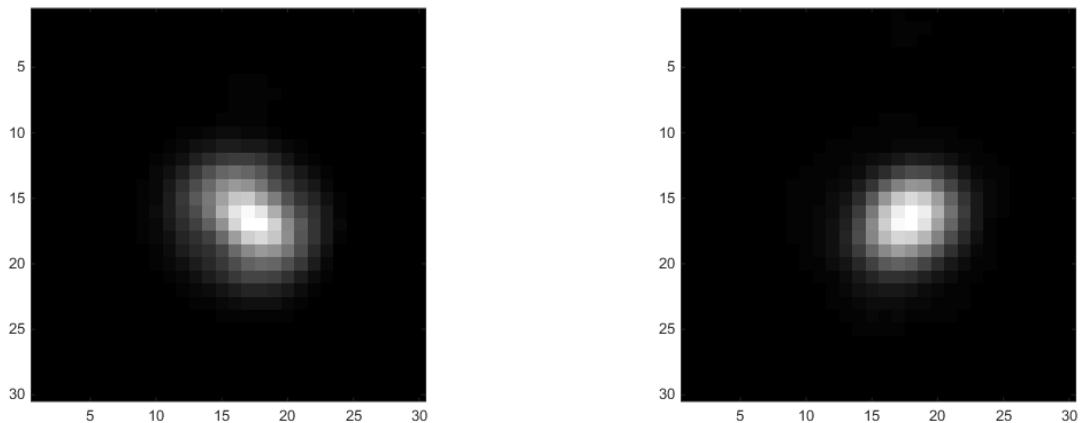


Figure 9. 30 x 30 pixel region from the PSM on two sides of focus from the center of curvature of a small tooling ball. The slightly elongated line shape with orthogonal directions the two sides of focus is the result of astigmatism in the PSM.

A small amount of astigmatism is evident in the images above from the PSM. The origin of this aberration is power in a plate beam splitter, which is at 45 degrees to the collimate point source. While the images below from the W2 looking on opposite sides of focus show much better rotational symmetry than the PSM and even show the on-axis zero for  $\sim 1 \lambda$  of defocus at the detector. The PSM is marginally easier to focus on the pinhole due to the astigmatism. The W2 and its better image quality suggests that looking at the on-axis zero could lead to improved performance. This is especially true considering that the defocus motion is effectively double-pass since the source and detector are both moved.

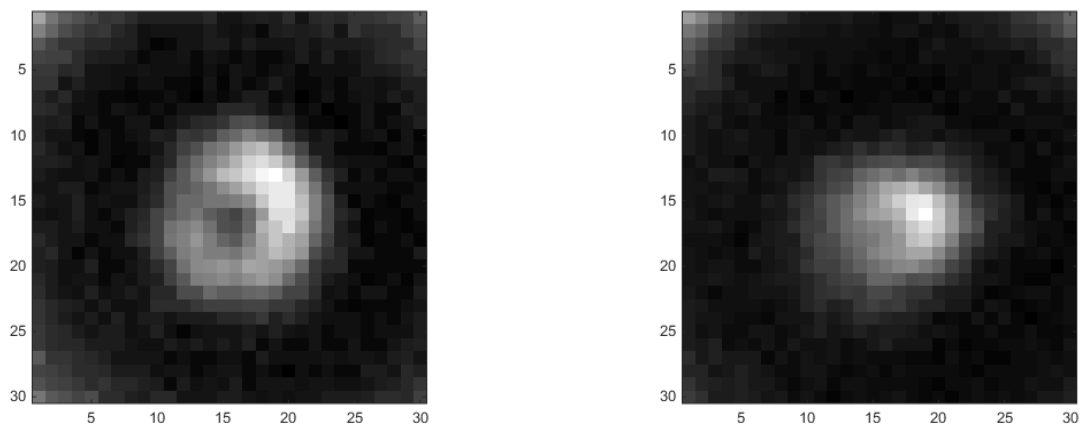


Figure 10. 30 x 30 pixel region from the W2 on two sides of focus from the center of curvature of a small tooling ball. The image on the left shows the on-axis zero from defocus. Contrast was stretched in these images rather than adjusting exposure before recording, which would reduce the noise to a level comparable to Figure 9.

### 3.4 Ease of use

As a practical matter, the extended source and target of the W2 facilitates rapid initial alignment. This is because the circular aperture provides a large object in the FOV that can be seen in an image even when poorly focused and provides guidance as to direction to move. The following images hint at this possibility while looking at the tooling ball used above.

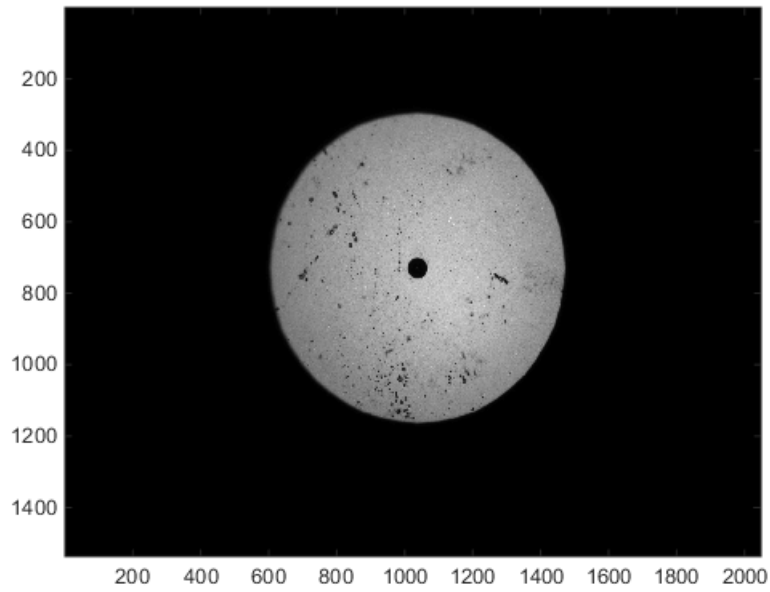


Figure 11. W2 image of tooling ball surface

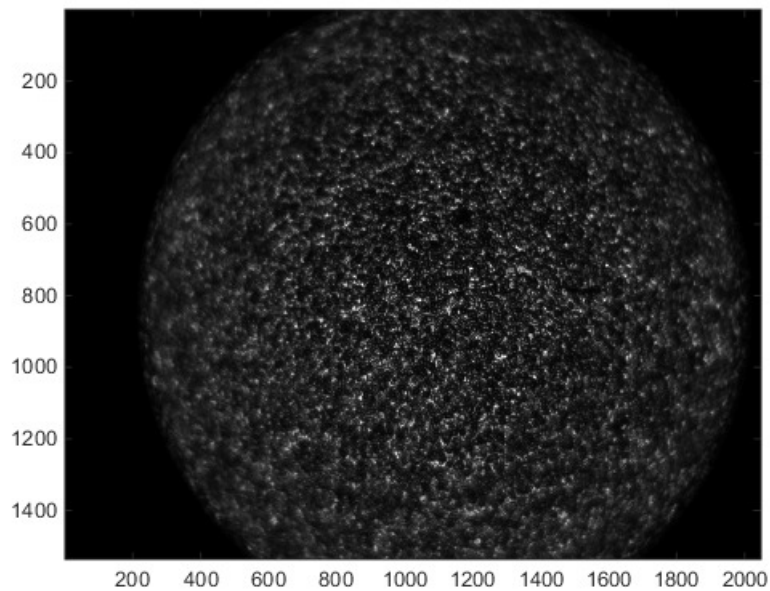


Figure 12. W2 image of internal diffuser that appears when moving from tooling ball surface to the center of curvature.

As one moves from the surface to the center of curvature of the tooling ball, a very short radius convex mirror, an image of the diffuser is clear observed. As one continues to the center of curvature, it is easily found because the large disk that is imaged gives clear guidance rather than a small spot that disappears.

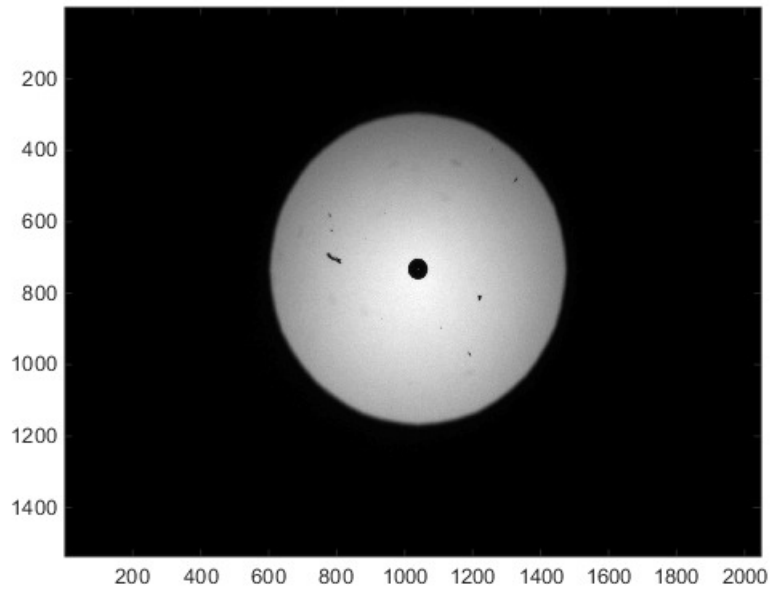


Figure 13. W2 image of tooling ball center of curvature.

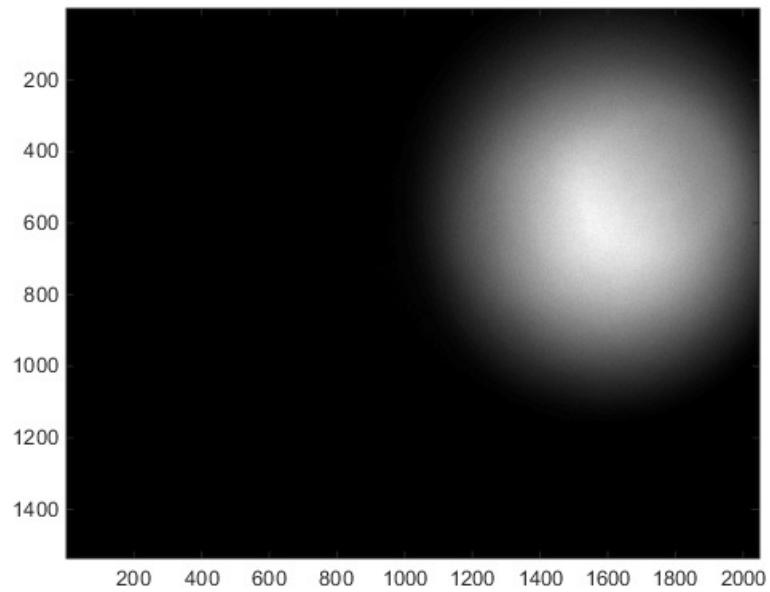


Figure 14. W2 image that is significantly out of focus, but still providing guidance to find the spot.

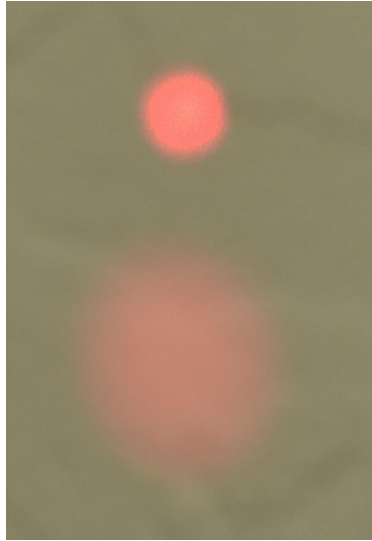


Figure 15. PSM spot on top (brighter and smaller) and W2 spot on the bottom on a wall with room lights on.

The picture above shows two spots. The smaller, brighter red spot is from a PSM and the larger, not quite as bright spot is from a W2. The picture was taken in normal office lighting. The background is actually a white wall that appears darker so as to reveal the differences between the two spots. Regardless of those details, both spots are easily visible in normal office lighting.

The W2 power output with the standard red LED is  $50 \mu\text{W}$  compared to a  $132 \mu\text{W}$  for the rather old PSM (S/N 1) used in this experiment. The larger beam size is also apparent; however, one must consider that the W2 is projecting an image. Specifically, the image below uses a DSLR to act as an eye and look into the W2 collimator. Clearly, the W2 is projecting an image of the reticle. It is also clear that a different color LED could be easily substituted for the red one used here. In any case, the W2 LED is easily visible on a wall.

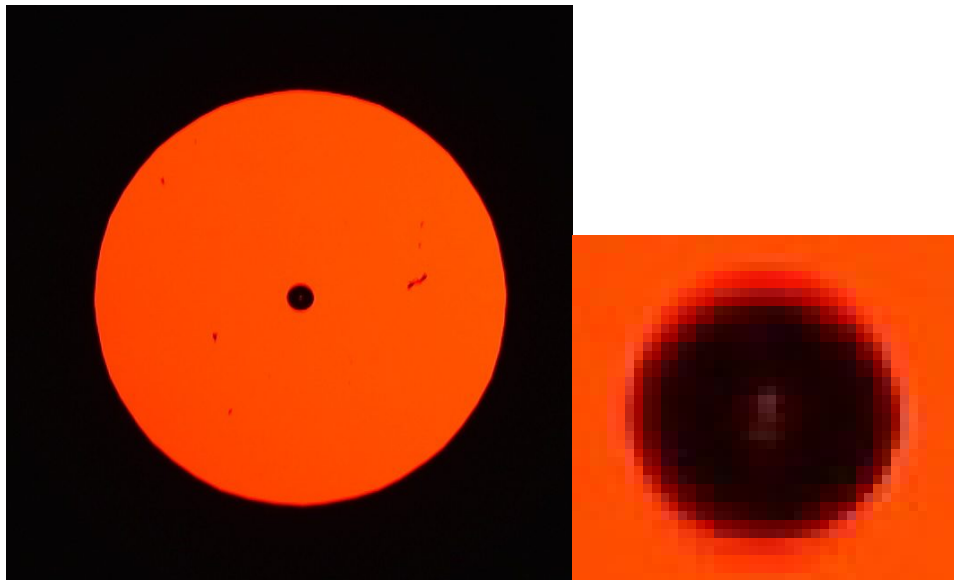


Figure 16. Portions of a DSLR image (60 mm, F/2.8 lens) taken looking into W2 collimator output.

#### **4. SUMMARY AND CONCLUSION**

As already stated, in practical terms, both the PSM and W2 will often be limited in performance by fixtures and the environment. However, the W2 does have improved statistics for centroid measurements compared to the PSM with the simplistic processing implemented for this paper. The W2 also has the potential for improved axial repeatability using the edge of the obscuration. In both cases, more sophisticated analysis techniques may further improve performance.

In addition to the basic performance improvement present in the W2, there are a range of improvements in ease-of-use and adaptability of a practical nature that should prove useful.

#### **REFERENCES**

- [1] Parks, R. E., and Kuhn, W. P., "Optical alignment using the Point Source Microscope," Proc. SPIE 5877, (2005).
- [2] Smith, W. J., [Modern Lens Design], McGraw-Hill Inc., New York, 20 (1992).